Contents

1
Numerical results for the clock model

We present results of scaling in bond dimension and system size with the CTMRG algorithm for the five- and six-state clock model.

1.1 Introduction

In the field of phase transitions and critical phenomena, the two-dimensional topological phase transition discovered by Kosterlitz and Thouless [1, 2] receives much attention. This phase transition is characterized not by an order parameter which indicates a breaking of symmetry, but by the proliferation of topological defects.

In the low-temperature phase, the two-point correlation functions decay with a power-law with varying exponent $\eta(T)$. At the transition, the correlation length diverges as

$$\xi \propto \exp(A|T - T_c|^{-1/2}), \tag{1.1}$$

with A a non-universal constant. Above the transition, the two-point correlators decay exponentially.

The XY model consists of planar rotors on the square lattice. It exhibits the Kosterlitz-Thouless (KT) phase transition and by the Mermin-Wagner-Hohenberg theorem the symmetry of the ground state is broken for all temperatures, due to the $O(2)$ (planar rotational) symmetry of the potential [3, 4].

The q-state clock model possesses the discrete $\mathbb{Z}_q$ symmetry and is an interpolation between the Ising model, which corresponds to $q = 2$, and the XY model, which corresponds to $q \to \infty$. Its energy function is given by

$$H_q = -\sum_{\langle ij \rangle} \cos(\theta_i - \theta_j), \tag{1.2}$$

with the spins taking the values

$$\theta = \frac{2\pi n}{q} \qquad n \in \{0, \ldots, q-1\}. \tag{1.3}$$

It has been proven that for high enough q, this model indeed exhibits a Kosterlitz-Thouless transition [5]. Furthermore, it has been proven that for $q \geq 5$, a general model with $\mathbb{Z}_q$ symmetry (of which Eq. 1.2 is a special case) has three phases: a symmetry broken phase for $T < T_1$, an intermediate phase with power law decay of the correlation function, and a high-temperature phase with exponential decay of the correlation function for $T > T_2$ [6].

In the Villain formulation of the potential [7], it has been proven that the transition at T_2 is a BK-transition [8], and numerical results suggest that for a broad range of temperatures, the thermodynamic behaviour becomes identical to the XY model for high enough q [9].

Furthermore, in the Villain formulation it is known that [10, 11]

$$\eta(T_1) = \frac{4}{q^2}, \qquad \eta(T_2) = \frac{1}{4}, \tag{1.4}$$

where η is the spin-spin correlation function exponent. In CTMRG simulations, it is possible to obtain this exponent through the relation

$$\frac{\eta}{2} = \frac{\beta}{\nu}, \tag{1.5}$$

where the fraction $\frac{\beta}{\nu}$ is found by finite-size scaling of the magnetization (see ??).

For the cosine model in Eq. 1.2, the value q_c for which it first exhibits a BK-transition is not precisely known. There is some disagreement about whether the cases $q = 5, 6$ exhibit KT-type transitions (see previous numerical results below).

In our simulations we will focus on the cases $q = 5, 6$, to (i) study the nature of the phase transition from the new perspective provided by the corner transfer matrix formalism and (ii) compare the accuracy of finite-m and finite-N scaling within the CTMRG method to other established numerical methods.

We briefly summarise previous numerical results, then present results obtained with the CTMRG algorithm.

1.2 Previous numerical results

1.2.1 The $q = 5$ clock model

The general consensus is that the two transitions of the $q = 5$ clock model with cosine potential are of the KT-type, though there are no rigorous results. It is also assumed that the critical indices are the same as those in the Villain formulation.

The disagreement about the nature of the phase transitions stems from numerical results for the helicity modulus [12].

Most notably, Baek and Minnhagen [13] claim that since the helicity modulus does not vanish in the high-temperature phase, the upper transition is not of the KT-type.

It was shown by Kumano et al. in [14], however, that the definition used by Baek and Minnhagen is not suitable for systems with a discrete symmetry. The correct discrete definition yields the expected result, namely that the helicity modulus does vanish and the three-phase KT-picture holds.

The conclusion of Kumano et al, which was obtained by a Monte Carlo study, was verified by Chatelain [15] using the TMRG algorithm [16] (see also **??**). Chatelain also found that the critical indices match those of the Villain model (Eq. 1.4), implying the cosine model is in the same universality class as the Villain model.

After the rebuttal by Kumano et al., Baek et al. published another work [17] in which they again use the (in the eyes of Kumano et al.) wrong definition of the helicity modulus, yet calculated in a different way. Again they conclude the transition is not of the KT-type.

Meanwhile, Borisenko et al. [18] carried out a very detailed Monte Carlo study confirming the KT-picture, using Binder-cumulants to find the critical points and the magnetization and susceptability to find the critical indices.

Brito et al. [19] conclude from a Monte Carlo study that while the transition is of KT-type, the resolution of their numerical method is not high enough to distinguish between T_1 and T_2.

Table 1.1 shows the results for the transition temperatures found by other authors.

1.2.2 The $q = 6$ clock model

Here, there is overwhelming consensus that both transitions are of the KT-type. The only exceptions are Lapilli et al. [9] and Hwang [20].

Lapilli et al. use the incorrect definition of the helicity modulus.

	T_1	T_2
Brito et al.[1] (2010) [19]	0.91	0.90
Borisenko et al. (2011) [18]	0.9056	0.9432
Kumano et al. (2013) [14]	0.908	0.944
Chatelain (2014) [15]	0.914	0.945
This work (finite-N scaling)	0.915	0.935
This work (finite-m scaling)	-	0.944

Table 1.1: Previous results for the transition temperatures for $q = 5$.

	T_1	T_2
Tomita and Okabe (2002) [22]	0.7014	0.9008
Hwang[2] (2009) [20]	0.632	0.997
Brito et al. (2010) [19]	0.68	0.90
Kumano et al. (2013) [14]	0.700	0.904
Krčmár et al. (2016) [21]	0.70	0.88
This work (finite-N scaling)	0.700	0.883
This work (finite-m scaling)	-	0.901

Table 1.2: Previous results for the transition temperatures for $q = 6$.

Hwang asserts that the transition is not of KT-type because the data, which was obtained from systems of rather small size ($L \times L$-systems with $L = 20, \ldots, 28$), also agrees with a power-law divergence of the correlation length. We will get back to this point.

The previous results for the transition temperatures are listed in Table 1.2. For an overview that goes further back, see [21].

We note that [14, 19, 22] use Monte Carlo methods, while [21] uses the CTMRG algorithm (combined with finite-size scaling, but not with finite-m scaling).

[1] These authors found $T_1 > T_2$, which is not an error in the text, but due to the low resolution of the methods used.

[2] To obtain these values, the author assumed an algebraic divergence of the correlation length.

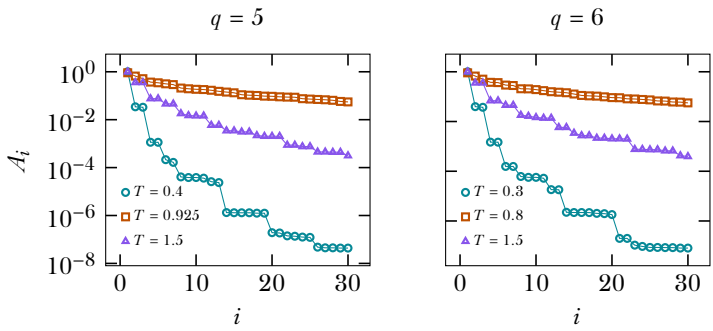

Figure 1.1: First part of the spectrum of A with fixed boundary, calculated with $m = 100$ and a convergence threshold of 10^{-8}, at temperatures corresponding to the ordered phase, approximate midpoint of the massless phase and disordered phase, respectively.

1.3 Spectrum of the corner transfer matrix

In order to get an idea of the accuracy that we might expect, we have plotted the spectrum of the $q = \{5, 6\}$ clock models in Fig. 1.1.

It is clear that the spectra of both clock models fall off at about the same pace, if we compare points in the ordered, massless and disordered phase. The $q = 6$ clock model has a slightly more degenerate spectrum, as might be expected from its larger symmetry group, but there is no clear pattern.

As compared to the Ising model (see ??), the spectra of the $q = \{5, 6\}$ clock models fall off much more slowly[3]. This implies that a much larger bond dimension is needed to obtain the same accuracy for quantities in the thermodynamic limit.

[3]For the calculation of the spectrum of the Ising model in this work, a bond dimension of $m = 250$ was used, as opposed to $m = 100$ for the clock model. This means that, in small part, the slower decay of the spectrum is due to the normalization $\mathrm{Tr}\, A^4 = 1$. But this does not change the general picture that the spectra of the $q = \{5, 6\}$ clock models decay more slowly.

1.4 Magnetization

For the clock model, we define the magnetization per site as

$$M = \langle \cos \theta_0 \rangle, \tag{1.6}$$

where θ_0 is the central spin.

This quantity can be computed in the same way as for the Ising model (see ??) by generalizing the tensor b_{ijkl} to

$$b_{ijkl} = \sum_{n \in \{0,\ldots,q-1\}} \cos\left(\frac{2\pi n}{q}\right) \delta_{nijkl}. \tag{1.7}$$

1.5 Classical analogue to the entanglement entropy

The classical analogue to the half-chain entanglement entropy S is defined in ??. Its definition remains valid.

In the limit $T \to \infty$, for both a fixed and free boundary, we have

$$S(T \to \infty) = 0. \tag{1.8}$$

To see this, consider that all 2^{2N} configurations on the inner edges of the $N \times N$ quadrant represented by the corner transfer matrix are equally likely in this limit, hence

$$A_{ij} = \frac{1}{2^{2N}}, \tag{1.9}$$

which has one eigenvalue of 1 and the others 0[4].

In the limit $T \to 0$, there is only one non-zero matrix element in the case of a fixed boundary (namely all inner spins having the same value as the outer boundary), and q equally likely configurations in the case of a free boundary, yielding

$$S^{\text{fixed}}(T = 0) = 0,$$
$$S^{\text{free}}(T = 0) = \log q.$$

[4] One can also make the argument that the corresponding quantum state tends to a product state in the limit $T \to 0$, yielding the same conclusion.

For a fixed boundary, the point of maximum entropy approaches the massless phase from the high-temperature region, hence tending towards T_2. In contrast, the point of maximum entropy approaches T_1 for systems with a free boundary.

Maybe make intuitive why?

Fig. 1.2 and Fig. 1.3 show these quantities for $q = 5$ and $q = 6$ for systems with a fixed boundary, clearly confirming the three-phase picture.

1.6 Transition temperatures

Since we expect an essential singularity of the form in Eq. 1.1 for both transitions, for finite systems we have

$$N = a \exp\left(b|T^\star(N) - T_c|^{-1/2}\right), \tag{1.10}$$

where N is an effective finite length scale of the system and a and b are non-universal constants.

N is the system size in the case of finite-size scaling and a length scale derived $\xi(m)$ from the bond dimension m in the case of finite-m scaling. Throughout this chapter, we have defined $\xi(m)$ through the relation

$$S \propto \frac{c}{6} \log \xi(m) \tag{1.11}$$

where $c = 1$ is expected, since the massless phase corresponds to a Gaussian model [2]. These assumptions are validated in section 1.7.1.

We define $T^\star(N)$ as the point of maximum entanglement entropy, as discussed in ??.

Inverting Eq. 1.10 gives the following relations for the pseudocritical transition temperatures

$$T_1^\star(N) = -\frac{\alpha_1}{(\log \beta_1 N)^2} + T_1 \tag{1.12}$$

$$T_2^\star(N) = \frac{\alpha_2}{(\log \beta_2 N)^2} + T_2 \tag{1.13}$$

where $\alpha = b^2$ and $\beta = 1/a$ (we drop the subscripts denoting the transition).

For convenience, we define the scaled length variable

$$\ell = (\log \beta N)^2, \tag{1.14}$$

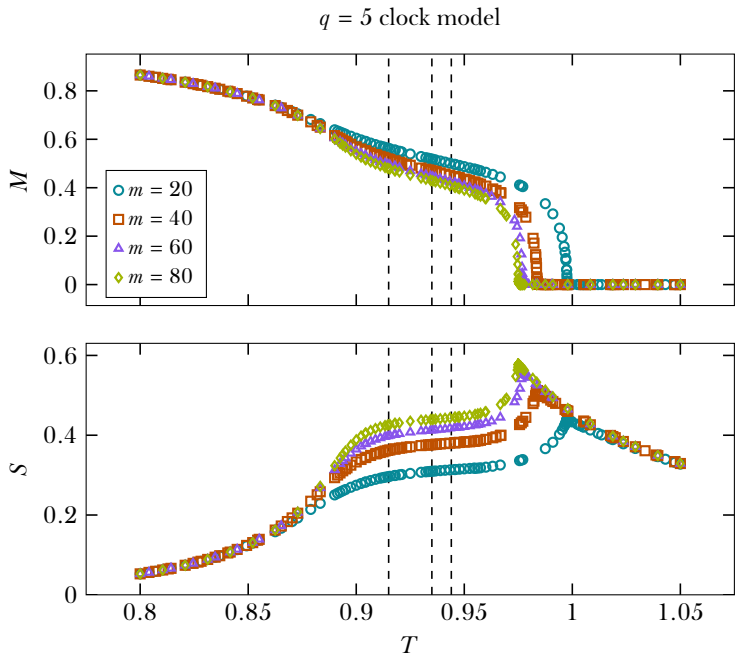

Figure 1.2: Classical analogue to half chain entanglement entropy (??) and magnetization (Eq. 1.6) computed for systems with a fixed boundary for the $q = 5$ clock model. Simulations were done with a convergence threshold of 10^{-7}. The dashed lines denote the transition temperatures found in this study.

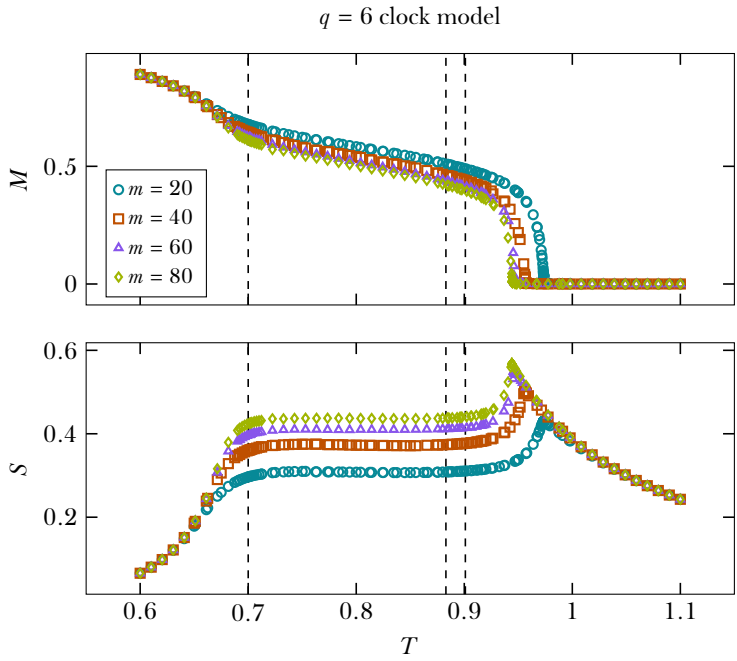

Figure 1.3: Classical analogue to half chain entanglement entropy (??) and magnetization (Eq. 1.6) computed for systems with a fixed boundary for the $q = 6$ clock model. Simulations were done with a convergence threshold of 10^{-7}. The dashed lines denote the transition temperatures found in this study.

such that

$$T^{\star}(N) - T_c \propto \frac{1}{\ell}. \tag{1.15}$$

1.6.1 Numerical difficulties with finite-m simulations around T_1

For both the $q = \{5, 6\}$ clock models, it has been found that locating $T_1^{\star}(m)$ is not possible, since for systems with a free boundary, numerical errors cause the matrices A and P to lose their symmetry and converge to a fixed boundary fixed point instead. This happens after a modest amount of steps, especially near $T_1(m)^{\star}$, making it impossible to reach any feasible convergence threshold such as 10^{-6}.

This means that for locating T_1, we must rely on finite-size scaling, whereas for locating T_2 we can rely on both finite-size and finite-m scaling.

1.6.2 Transition from the ordered to the massless phase T_1

Fig. 1.4 and Fig. 1.5 show the fits to Eq. 1.10 for $q = \{5, 6\}$, yielding

$$T_1^{q=5} = 0.915, \qquad T_1^{q=6} = 0.700. \tag{1.16}$$

Conform to the Kosterlitz-Thouless divergence of the correlation length, the pseudocritical temperatures indeed become linear in $\frac{1}{\ell}$, with ℓ defined in Eq. 1.14.

It is interesting to note that finite-size effects are much more pronounced for $q = 5$.

1.6.3 Transition from the massless to the disordered phase T_2

1.6.3.1 Finite-size scaling

Finite-size scaling, shown in Fig. 1.6 for $q = 5$ and Fig. 1.8 for $q = 6$ yields

$$T_2^{q=5} = 0.935, \qquad T_2^{q=6} = 0.883. \tag{1.17}$$

For both clock models, finite-size effects are large. For $q = 6$, the finite-size effects are more pronounced than at T_1.

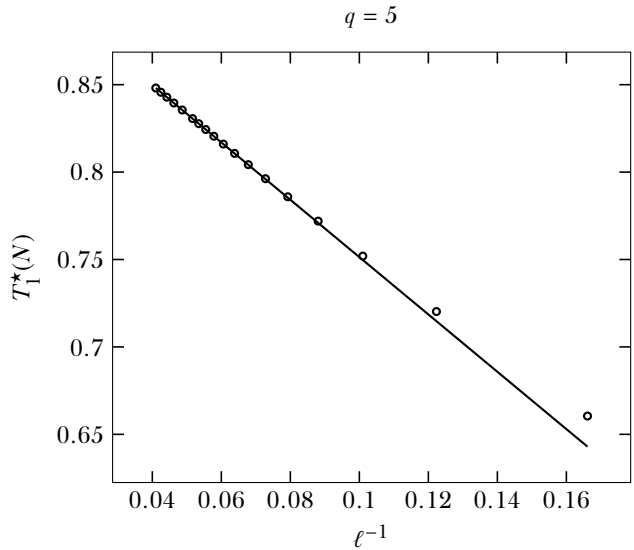

Figure 1.4: We find $T_1 = 0.915$ for the $q = 5$ clock model. We have fitted the final 8 points $n = \{60, 65, 70, 80, 90, 100, 110, 120\}$. Not included in the fit are $n = \{10, 15, \ldots, 55\}$. m was chosen such that the truncation error was smaller than 10^{-6} for $n \leq 70$ and smaller than 10^{-5} for $n > 70$. In finding the maximum of the entropy, a tolerance in temperature of 10^{-5} was used.

1.6.3.2 Finite-m scaling

Finite-m scaling, shown in Fig. 1.7 for $q = 5$ and Fig. 1.9 for $q = 6$ yields

$$T_2^{q=5} = 0.944, \qquad T_2^{q=6} = 0.901. \tag{1.18}$$

It is seen that with finite-m simulations, systems of significantly larger effective size can be simulated. From the finite-size fits to $T_2^\star(N)$, it can be estimated that a system of $m = 90$ approximately corresponds to a 2700×2700 lattice for $q = 5$ and a 2400×2400 lattice for $q = 6$.

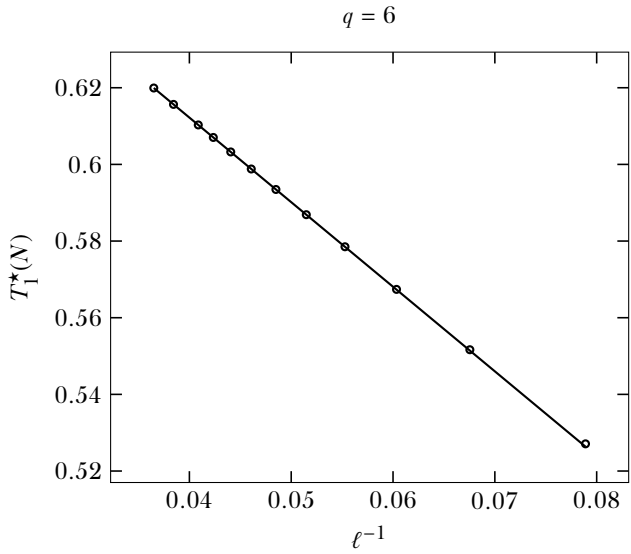

Figure 1.5: We find $T_1 = 0.700$ for the $q = 6$ clock model. We have fitted the final 8 points $n = \{35, 40, 45, 50, 55, 60, 70, 80\}$. Not included in the fit are $n = \{15, 20, 25, 30\}$. m was chosen such that the truncation error was smaller than 10^{-6} for $n \leq 60$ and smaller than 10^{-5} for $n > 60$. In finding the maximum of the entropy, a tolerance in temperature of 10^{-5} was used.

There is some structure in the data, but as long as a wide range of m values is included, the estimation of T_2 is robust.

1.7 The massless phase

1.7.1 Central charge

By fitting the relation in Eq. 1.11, where $\xi(m)$ is calculated as in ??, we can directly extract the central charge in this region.

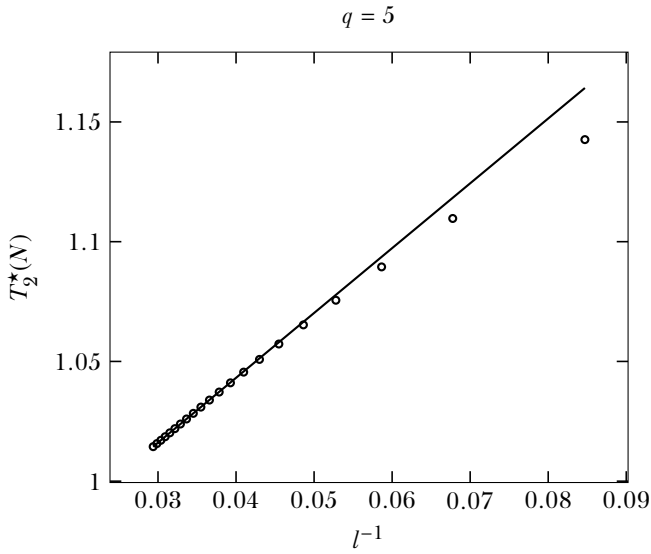

Figure 1.6: We find $T_2 = 0.935$ for the $q = 5$ clock model with finite-size scaling. We have fitted the final 6 points $n = \{85, 90, \ldots, 110\}$. m was chosen such that the truncation error was smaller than 10^{-6}. In finding the maximum of the entropy, a tolerance in temperature of 10^{-6} was used.

The result is shown in the top panel of ??. It is seen to precisely agree with $c = 1$ in the massless phase.

Outside the massless phase, a good fit to Eq. 1.11 can no longer be obtained. This is consistent with the location of T_1 and T_2 that are found in this work.

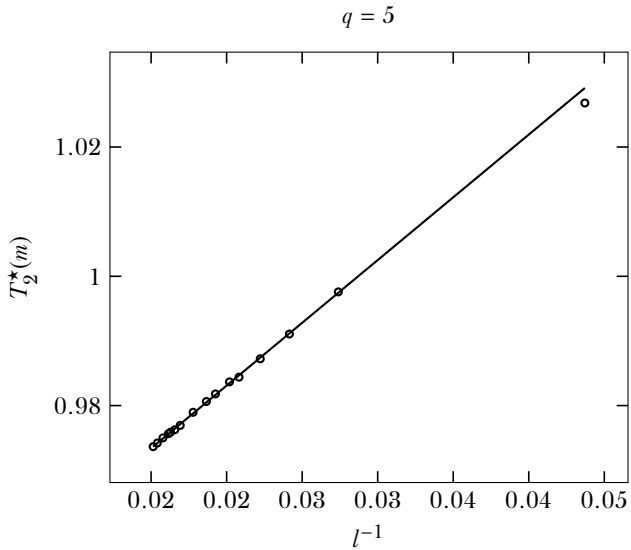

Figure 1.7: For the finite-m simulations, the fit yields $T_2 = 0.944.$ using $m = 20, 25, \ldots, 90$ with a convergence threshold of 10^{-7}. The pseudocritical temperature belonging to $m = 10$ is also shown, but is not included in the fit.

1.7.2 Varying exponent for the magnetization

We may verify the exponent with which the magnetization goes to zero in the massless phase by fitting

$$M(m, T) = \xi(m)^{-\frac{\eta(T)}{2}}, \tag{1.19}$$

with $\xi(m)$ again defined via Eq. 1.11.

The result is shown in the middle panel of ??. It agree very well with bla bla. Refer to villain exponents.

Finish this when T_1 is definite

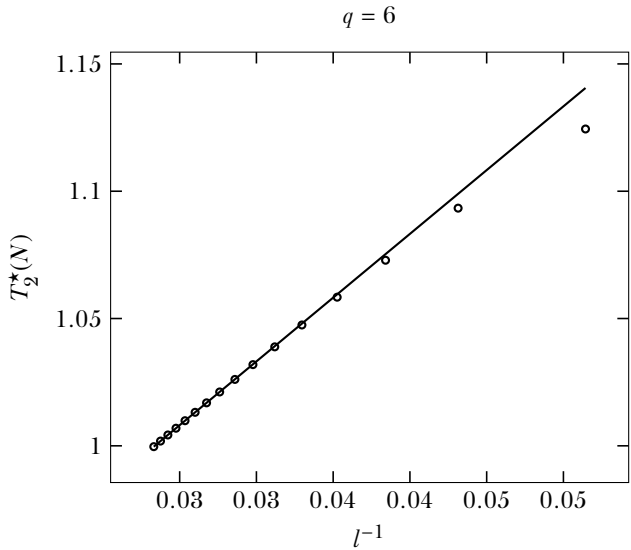

Figure 1.8: We find $T_2 = 0.883$ for the $q = 6$ clock model with finite-size scaling. We have fitted the final 6 points $n = \{60, 65, \ldots, 85\}$. The points $n = \{10, 15, \ldots, 55\}$ were not included. m was chosen such that the truncation error was smaller than 10^{-6}. In finding the maximum of the entropy, a tolerance in temperature of 10^{-6} was used.

1.8 Discussion

1.8.1 Finite-size effects

Overall, the values of T_1 and T_2 for $q = \{5, 6\}$ in this work agree well with the values found by other authors, see Table 1.1 and Table 1.2.

Finite-size scaling within the CTMRG is suffers more from finite-size effects than finite-m scaling, since smaller system sizes are accessible. It is plausible that this is the reason that finite-size scaling yields values that differ somewhat from previous results and the results of finite-m scaling.

There are two straightforward ways that might improve the finite-size re-

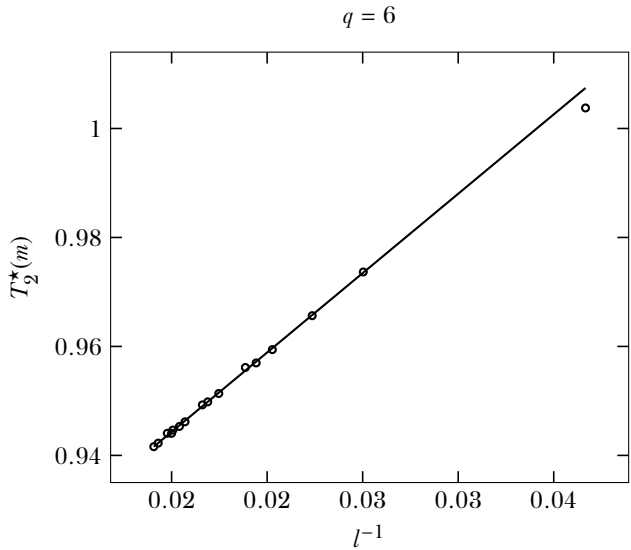

Figure 1.9: For the finite-m simulations, the fit yields $T_2 = 0.901.$ using $m = 20, 25, \ldots, 90$ with a convergence threshold of 10^{-7}. The pseudocritical temperature belonging to $m = 10$ is also shown, but is not included in the fit.

sults. The first is to systematically study how the chosen bond dimension (and correspondingly, the truncation error) influences the precision of the pseudocritical point. A start with this has been made in ?? for the Ising model. It might be possible to simulate larger system sizes without much loss of accuracy, but it seems unlikely that the same system sizes as in the finite-m regime are accessible. Furthermore, for finite-m results it is much easier to assess the convergence of quantities (see ??).

However, finite-size data is of much higher quality than the finite-m data, since the latter suffers from structure due to the spectrum of the corner transfer matrix. Therefore, it is not unlikely that results might improve if correction to scaling terms are included in the fits.

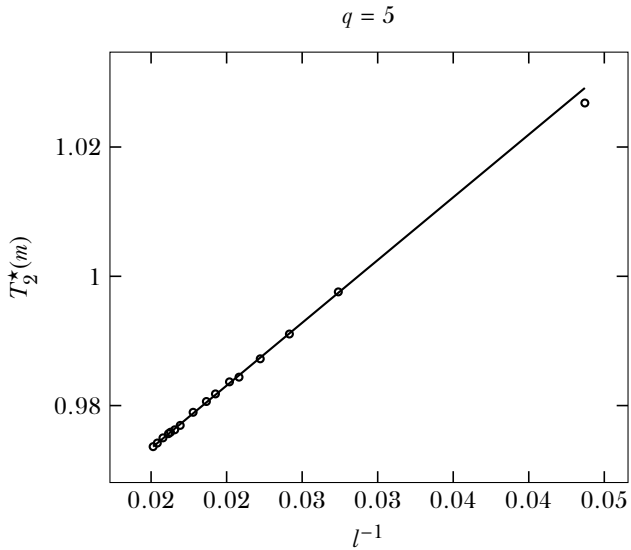

Figure 1.10: For the finite-m simulations, the fit yields $T_2 = 0.944.$ using $m = 20, 25, \ldots, 90$ with a convergence threshold of 10^{-7}. The pseudocritical temperature belonging to $m = 10$ is also shown, but is not included in the fit.

1.8.2 Other means of studying the transitions T_1 and T_2

In this study, we have used the point of maximum entanglement entropy as a definition of the pseudocritical point. The most obvious drawback of this method is that locating T_1 is not possible with finite-m simulations, as described in section 1.6.1. Finite-size simulations near T_1 are possible, but costly, since the spectrum of the corner transfer matrix decays slowly for systems with a free boundary.

A different way of finding T_1 is through the higher order parameters

$$M_a = \langle e^{ia\theta_0} \rangle, \tag{1.20}$$

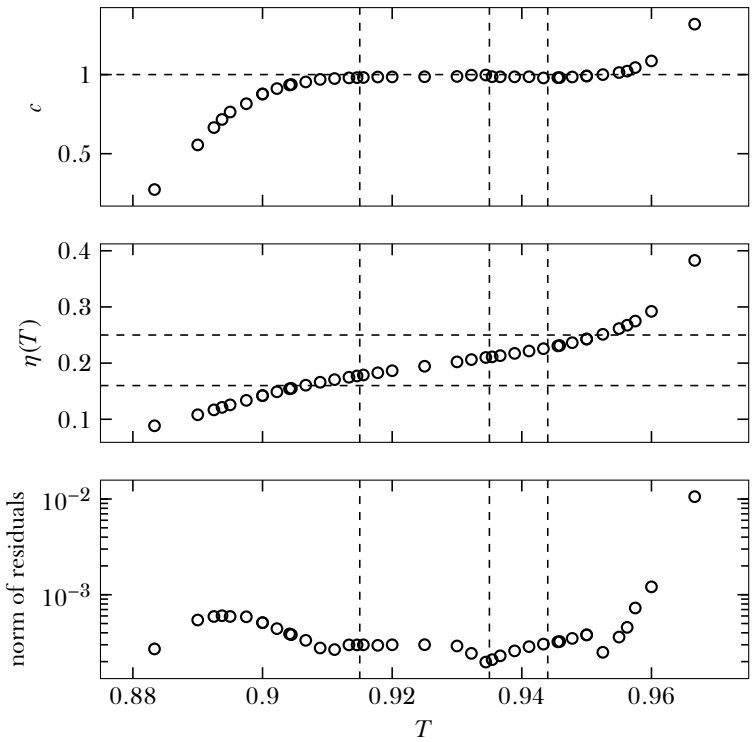

Figure 1.11: $\eta = \frac{2\beta}{\nu}$ reaches $\frac{4}{25}$ around $T = 0.906$ and $\frac{1}{4}$ around $T = 0.952$. First 4 values were left out of the fit.

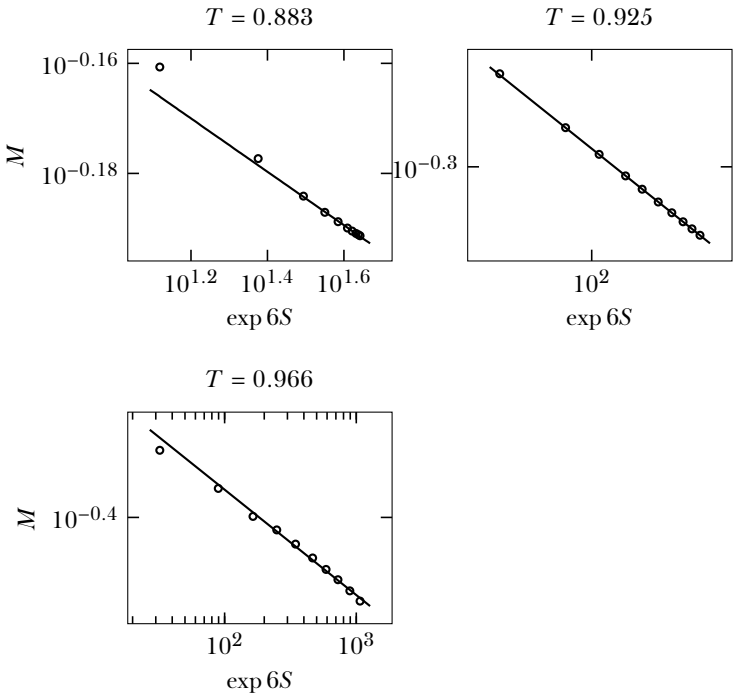

Figure 1.12: Fits to Eq. 1.19 for temperatures a little bit to the left of, in the middle of and a little bit to the right of the massless phase, respectively.

which should obey

$$|M_a| \propto \exp\left(-Ca^2/(T_1 - T)^{1/2}\right), \tag{1.21}$$

with C a non-universal constant [6].

M_a is readily obtainable with the CTMRG method and does not require a free boundary. However, it is not clear if this will increase the precision of T_1.

The transition T_2 may also be found by studying the magnetic susceptibility, as was done by [18]. The susceptibility diverges more strongly than the entropy, but requires numerical derivatives to find. It is plausible that this method would yield an accuracy comparable to the current method, since it requires the same simulations to obtain T_2. Nonetheless, it would serve as a good consistency check.

- use susceptibility at T_2 (like Borisenko)
- use finite-size corrections for exponent η, though this would probably require finite-size scaling as opposed to finite-m scaling.
- at T_1, it might be feasible to use the higher order parameters M_n to verify the dependence on n.
- second-order phase transition impossible with varying exponent.
- how does effective central charge diverge from 1 outside massless phase? This is not clear
- doesn't apparently make sense to take many consecutive m-values. Rather take sparse, but bigger m-values.
- For finite-N: tradeoff between truncation error and finite-size effects are not clear.
- finite-χ reaches much bigger system sizes, but has structure that needs to be overcome while fitting.
- fix bug where I attached an a-tensor with wrong temperature.
- omitting m values seems to give worse results than just taking them all, except for the really small ones.
- second-order phase transition cannot be ruled on grounds of this data, but is there theory that forbids it?

- If you make convergence too low, it can get impossible to reach, even for fixed boundary?

Bibliography

[1] J. M. Kosterlitz, and D. J. Thouless, "Ordering, metastability and phase transitions in two-dimensional systems", Journal of Physics C: Solid State Physics **6**, 1181 (1973).

[2] J. M. Kosterlitz, "The critical properties of the two-dimensional xy model", Journal of Physics C: Solid State Physics **7**, 1046 (1974).

[3] N. D. Mermin, and H. Wagner, "Absence of ferromagnetism or antiferromagnetism in one-or two-dimensional isotropic Heisenberg models", Physical Review Letters **17**, 1133 (1966).

[4] P. C. Hohenberg, "Existence of long-range order in one and two dimensions", Physical Review **158**, 383 (1967).

[5] J. Fröhlich, and T. Spencer, "The Kosterlitz-Thouless transition in two-dimensional abelian spin systems and the Coulomb gas", Communications in Mathematical Physics **81**, 527–602 (1981).

[6] J. Cardy, "General discrete planar models in two dimensions: duality properties and phase diagrams", Journal of Physics A: Mathematical and General **13**, 1507 (1980).

[7] J. Villain, "Theory of one-and two-dimensional magnets with an easy magnetization plane. II. the planar, classical, two-dimensional magnet", Journal de Physique **36**, 581–590 (1975).

[8] J. V. José, L. P. Kadanoff, S. Kirkpatrick, and D. R. Nelson, "Renormalization, vortices, and symmetry-breaking perturbations in the two-dimensional planar model", Physical Review B **16**, 1217 (1977).

[9] C. M. Lapilli, P. Pfeifer, and C. Wexler, "Universality away from critical points in two-dimensional phase transitions", Physical Review Letters **96**, 140603 (2006).

[10] S. Elitzur, R. B. Pearson, and J. Shigemitsu, "Phase structure of discrete abelian spin and gauge systems", Physical Review D **19**, 3698–3714 (1979).

[11] B. Nienhuis, "Critical behavior of two-dimensional spin models and charge asymmetry in the Coulomb gas", Journal of Statistical Physics **34**, 731–761 (1984).

[12] M. E. Fisher, M. N. Barber, and D. Jasnow, "Helicity modulus, superfluidity, and scaling in isotropic systems", Physical Review A **8**, 1111–1124 (1973).

[13] S. K. Baek, and P. Minnhagen, "Non-Kosterlitz-Thouless transitions for the q-state clock models", Physical Review E **82**, 031102 (2010).

[14] Y. Kumano, K. Hukushima, Y. Tomita, and M. Oshikawa, "Response to a twist in systems with Z_p symmetry: the two-dimensional p-state clock model", Physical Review B **88**, 104427 (2013).

[15] C. Chatelain, "DMRG study of the Berezinskii–Kosterlitz–Thouless transitions of the 2D five-state clock model", Journal of Statistical Mechanics: Theory and Experiment **2014**, P11022 (2014).

[16] T. Nishino, "Density matrix renormalization group method for 2D classical models", Journal of the Physical Society of Japan **64**, 3598–3601 (1995).

[17] S. K. Baek, H. Mäkelä, P. Minnhagen, and B. J. Kim, "Residual discrete symmetry of the five-state clock model", Physical Review E **88**, 012125 (2013).

[18] O. Borisenko, G. Cortese, R. Fiore, M. Gravina, and A. Papa, "Numerical study of the phase transitions in the two-dimensional $Z(5)$ vector model", Physical Review E **83**, 041120 (2011).

[19] A. F. Brito, J. A. Redinz, and J. A. Plascak, "Two-dimensional XY and clock models studied via the dynamics generated by rough surfaces", Physical Review E **81**, 031130 (2010).

[20] C.-O. Hwang, "Six-state clock model on the square lattice: Fisher zero approach with Wang-Landau sampling", Physical Review E **80**, 042103 (2009).

[21] R. Krčmár, A. Gendiar, and T. Nishino, "Phase transition of the six-state clock model observed from the entanglement entropy", arXiv:1612.07611 (2016).

[22] Y. Tomita, and Y. Okabe, "Probability-changing cluster algorithm for two-dimensional XY and clock models", Physical Review B **65**, 184405 (2002).